Journal of the Virtual Explorer, 2004
Volume 15
Paper 2
http://virtualexplorer.com.au/

Numerical simulation of disequilibrium structures in solid-melt systems during grain-growth

J. K. Becker

University of Mainz, Institute of Geoscience - Tectonophysic, Becherweg 21, 55099 Mainz, Germany

D. Köhn

University of Mainz, Institute of Geoscience - Tectonophysic, Becherweg 21, 55099 Mainz, Germany

N. Walte

University of Mainz, Institute of Geoscience - Tectonophysic, Becherweg 21, 55099 Mainz, Germany

M. Jessell

University of Toulouse, Laboratoire des Mecanism et Transfer Geologie, 38 rue des Trente-six Ponts, 31400 Toulouse cedex, France

P. D. Bons

University of Tübingen, Institute für Geologie und Paläontologie, Sigwartstr. 10, 72076 Tübingen, Germany

C. W. Passchier

University of Mainz, Institute of Geoscience - Tectonophysic, Becherweg 21, 55099 Mainz, Germany

L. Evans

University of Melbourne, School of Earth Sciences, Victoria 3010, Australia

Keywords: solid-melt, grain-growth, structures, disequilibrium, numerical simulation

Abstract: Numerical modeling is frequently used in, amongst other fields, geoscience to simulate a wealth of different geological mechanisms. Numerical models have the advantage that the model can be fully controlled and no unknown material properties or physical laws can influence the simulation.Therefore, numerical models are a superb method to test and enhance mechanisms or laws that have been deduced from observation of, or experiments with, natural rocks. In experiments or observations of natural rocks it is often difficult to recognize and/or estimate the influence of parameters that cannot be directly measured or controlled (such as stress/strain, heating/cooling, surface energies etc.).

In this paper we will present a method to simulate melting processes using numerical modeling. The simulations were performed to test the predicted behavior of solid-liquid systems with given surface energies and grain fabrics. Numerical modeling of partial melt microstructures is still at its beginning, but first results are very promising. A full control on the starting grain fabric and parameters such as the surface energies, and hence, the wetting angle or the mobility of boundaries is possible and all of these parameters can be easily changed. Furthermore, no unknown parameters or mechanisms can influence the simulation so the observed results must be directly related to the used algorithms. A set of simulations with varying surface energies, mobilities of boundaries and grain fabrics were performed that all yielded results that are in good agreement with observation on natural rocks, theoretical predictions and analogue experiments. One of the most important improvements on current theory, however, is that the wetting angle cannot be treated as constant, but rather changes over time to accommodate the gain or loss of melt in equilibrium and disequilibrium shaped melt pockets which influences the rheology of the solid-liquid system.

Table of Contents

Introduction

Melt processes, especially the existence of a three dimensional melt network, are of fundamental importance for melt migration and segregation, which is important in the upper mantle and the lower crust of the Earth [McKenzie, 1984; Scott and Stevenson, 1986; Sleep, 1988; Laporteet al., 1997; Rabinowitcz et al., 2001; Wark et al., 2003]. Furthermore, melt distribution and redistribution is a key factor in geological processes such as flow of (poly)crystalline aggregates or the homogenization of partial melts by chemical diffusion [Cooper et al., 1984; Laporte et al., 1997]. Many properties of systems with small amounts of melt depend on the distribution of the liquid phases at the grain scale. In high temperature experiments that were performed with major rock-forming minerals such as dunite + maficor ultramafic melt [Waff and Bulau, 1979; Hirth and Kohlstedt, 1995; Faul, 1997; Cmíral et al., 1998] or quartz + felsic melt [Jurewicz and Watson, 1984; Laporte, 1994; Laporte and Watson, 1995] apparent disequilibrium features were described that deviated from the predicted regular melt geometry:

1. fully wetted grain boundaries and melt lenses on grain boundaries
2. strongly distorted, melt-filled triple junctions
3. large, multigrain-bounded, melt pools.

These disequilibrium features where shown to have a potentially large impact on the porosity–permeability function of partially molten rocks, especially at low melt-fraction such as considered in the upper mantle [Faul, 1997; 2001]. It has been recognized that variations in grain size and crystal lattice–controlled surface-energy anisotropy modifies the actual liquid distribution in natural aggregates [Waff and Faul, 1992; Laporte and Watson, 1995; Jung and Waff, 1998; Wark et al., 2003]. The frequent observation of straight crystal facets of grains in contact with melt supports the latter explanation for nonequilibrium melt geometries [Waff and Faul, 1992; Hirth and Kohlstedt, 1995; Jung and Waff, 1998; Faul, 1997; Laporte and Provost, 2000]. Although quartz is considered to be more isotropic than olivine, all the above mentioned non-equilibrium features were observed in quartz + melt systems as well [Laporte, 1994; Laporte and Provost, 2000]. It is therefore important to study the liquid distribution in natural aggregates using experiments and/or numerical simulations. However, in experiments with natural rocks (HT-experiments), some of the main controlling parameters of melt processes cannot be measured or controlled and these experiments do not allow a continuous observation but rather, after quenching of the sample, show a snapshot of the process at the time of quenching (for examples of HT-experiments see [Tullis et al., 1973; Jurewicz and Watson, 1984; Hirth and Kohlstedt, 1995; Laporte and Watson, 1995; Faul, 1997] and references therein). This is insofar unsatisfying as the development of melt pockets and/or grain boundaries give valuable insights into the behavior of melt, its redistribution, development of non-equilibrium features and splitting or merging of non-equilibrium shaped melt pockets [Faul, 1997].

In situ experiments using analogue materials were performed to study the dynamic development of grain-boundary structures and melt segregation under deformation with a continuous observation of the experiment [Park and Means, 1996; Bauer et al., 2000; Rosenberg and Handy, 2000; Walteet al., 2003. Walte et al. (2003)] concentrate on influences of static grain growth on the development of disequilibrium structures in static systems and we will compare our results from numerical modeling of a static solid-liquid system with their experiments. They find that all previously observed disequilibrium-structures can develop due to the collapse of small grains during coarsening of the whole aggregate [Walte et al., 2003]. Using numerical modeling, we have additional control on important parameters like relative solid-solid and solid-liquid surface energies and are able to continuously observe the interacting processes and hence the evolution of melt pockets and grains.

Jessell et al. (2001) have introduced a numerical model called Elle that is based on a set of different modules each simulating one aspect of deformation or metamorphism of natural rocks on the grain scale. Here, we introduce an Elle-module that can be used to simulate melt processes at the grain scale. In this module, only the known and/or assumed physical laws for the distribution of a liquid-phase within a solid matrix are used and, in contrast to e.g. HT-experiments, different parameters are easily controlled or changed. Therefore, Elle is a superb tool to test and enhance the physical laws obtained from HT-experiments or, in more general terms, natural observations since it allows full control on all used parameters and the results cannot be

modified by unknown, or unconstrained material properties, geological or physical mechanisms and scaling problems.

Wetting angles and surface energies

In a partially molten, monomineralic system, the equilibrium melt distribution is characterized by a constant wetting angle whose value is a function of the surface energies of solid-solid boundaries(γ_{ss}) and solid-liquid boundaries (γ_{sl}) [Laporte et al., 1997]. The wetting angle can be easily calculated using relative surface energies from the following equation [Bulau et al. 1979]:

$$2\cos\left(\frac{\theta}{2}\right) = \frac{\gamma_{ss}}{\gamma_{sl}}$$

with γ as the wetting angle and γ_{ss} or γ_{sl} as solid-solid or solid-liquid surface energies respectively. If $0° < \gamma < 60°$, melt pockets have convex boundaries Figure 1a and an interconnected network of channels along grain edges exists, even for an infinitesimally small amount of melt [Bulau et al., 1979]. If $\Delta t > 60°$, the melt occurs as isolated concave pockets at grain corners Figure 1c [Laporte et al., 1979]. If $\Delta t = 60°$, the melt pocket has straight boundaries Figure 1b while with $\Delta t > 60°$ the melt pockets tend to have concave boundaries (Figure 1c) [Laporteet al., 1979].

Figure 1. Pictures of different stages during simulation 1a

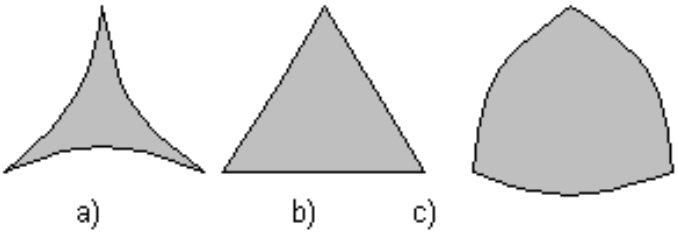

Shapes of melt pockets at different wetting angles:

a. $\gamma = 10°$
b. $\gamma = 60°$
c. $\gamma < 60°$

It has also been suggested (see [von Bargen and Waff, 1986; Laporte et al., 1997] and references therein) that the curvature of the solid-liquid interfaces is constant since it results from the wetting angle at solid-liquid interfaces.

The Numerical Model

As a starting grain fabric, the Elle code uses a set of polygons (called "flynns", Figure 2a) that can, for example, resemble grains in a thin section or an arbitrary designed (poly)crystalline aggregate in two-dimensions. These flynns carry information on the physical and chemical properties of a certain region. The vertices (nodes, Figure 1a) of the flynns can have additional physical and chemical properties. Furthermore, a set of unconnected nodes (called "unodes") can be introduced within the flynns that can be used to describe e.g. chemical variations or varying orientation of crystallographic axes throughout a flynn [Jessell et al., 2001]. All Elle-programs use such a topological description that is saved in a text-file that can be (automatically) translated from standard images (ppm, jpg, gif etc.). To avoid problems due to boundary reflections, the model wraps the boundaries so that the upper and lower and the left and right part are connected.

This data-set can be used to describe physical and chemical properties of a natural rock and the list of properties can easily be expanded as needed. Utilizing the respective physical laws for deformation and/or metamorphism, the data-set can be changed to reflect the evolution of a natural rock resulting from different competing processes. During the simulation, the change of the grain fabric over a certain small increment of time is achieved by moving the nodes of the flynns in small increments and constantly checking the validity of the topology and the correctness of the movement in terms of physical, chemical and geological laws.

The resolution in space is user defined and describes the distance between two or three nodes during the simulations. In Elle this is called the "switch distance" meaning that nodes are inserted or deleted if the distance between two (or three) neighboring nodes falls below or exceeds the switch distance. The switch distance also determines when a neighbor switch occurs when two grains approach each other. If the spacing between two neighboring nodes is smaller than the switch distance or greater than twice the switch distance, an action is taken (delete or insert nodes respectively). Parameters such as physical or geological properties for newly inserted nodes are calculated from the

two neighboring nodes. This maintains the desired constant resolution throughout the simulation. The switch distance influences the number of nodes and therefore recursively influences the time needed to simulate any given process. The more nodes in a simulation, the longer the calculations take and vice versa. It is desirable to balance the number of nodes and the required resolution of the simulation so that computation time is minimized. The movement of nodes is calculated with the general equation: $\Delta x = Fm\Delta t$ where Δx is the incremental displacement vector, F is the driving force vector, m is the mobility and Δt is the time increment. The magnitude of a displacement is thus proportional to the product of mobility and time increment. A change in mobility can thus be regarded as an effective change in Δt. The mobility can be adjusted as needed with values between 10^{-10} and 10^{-11}. The mobility influences the velocity but not the direction of node movement. In the presented simulations, high ratios of the mobility of boundaries of the melt pockets and the surrounding grains result in a faster movement of the boundary nodes while low ratios of these parameters result in a slower movement (see simulations 4 to 6). However, these values do not influence the final grain fabric so that the solution is stable and accurate enough within the chosen time resolution.

The movement of nodes and hence the change of the grain fabric in the Elle_melt module depends on the relative surface energy of solid-solid and solid-liquid surfaces. If a node movement decreases the free energy of a system, the node will be moved in the calculated direction (if topology-checks allow the movement). The direction of movement is determined in the following way (Figure 2b , see [Bons et al., 2001]): from the current node-position an arbitrary direction is chosen and the change of the total energy is calculated.From this arbitrary direction, 3 orthogonal directions are calculated and the change of the free energy is calculated. The total change in free energy of the system of all 5 positions (4 newly chosen ones and the current node position) is compared and the node is moved in the direction that decreases the free energy of the system the most.

Figure 2. General concept of an Elle file with flynns and nodes

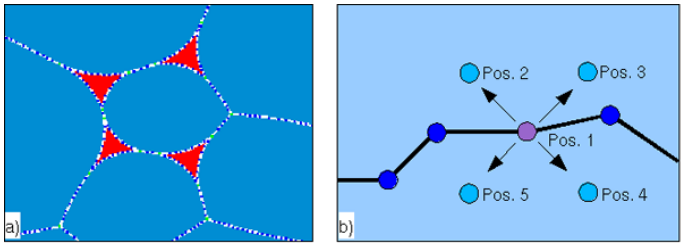

a. General concept of an Elle file with flynns and nodes. Each flynn and node can hold information on various parameters. In this example, the blue polygons resemble grains and the red polygons resemble melt pockets.
b. To decide if a node is moved and in which direction, four arbitrary new positions are chosen (Pos. 2 - 5). The resulting decrease or increase of the free energy of each node position (Pos. 1 - 5) is calculated and the position showing the highest decrease of the free energy is chosen.

Melt specific parameters

Different parameters influence the behavior of melt during experiments and simulations: surface energies, melt fraction and permeability of the rock. In our simulations the permeability is set to infinity so that different melt pockets can freely interact and diffusion is not rate-limiting. We effectively assume that there is a three-dimensional connectivity between melt pockets on the thin-section scale that we model.

In the Elle_melt module, the melt fraction can be easily adjusted. The starting grain fabric for a simulation includes information about the grains and melt pockets, the ratio of the area of melt and area of grains is the melt fraction. Using parameters at program start-up, this melt fraction can be fixed to the starting value or it can be decreased or increased during the simulations. During a simulation, the current melt fraction is constantly compared to the desired melt fraction. If it is the same or the melt fraction is allowed to increase without bounds, the melt fraction does not influence the calculations at all. If the melt fraction is outside the desired range, node-movements that adjust the current melt fraction towards the desired one are preferred. The melt experiments shown below all use the starting melt fraction as a fixed value.

In the Elle_melt module, the surface energies of solid-solid boundaries (Δt_{ss}), solid-liquid boundaries (Δt_{sl}) and liquid-liquid boundaries (Δt_{ll}) can be adjusted.

Liquid-liquid boundaries (Δt_{ll}) have no physical meaning, since melt composition is always the same. They may however occur in the models for topological reasons, whereby their surface energy is set to zero. Solid-solid surface energies are set to unity and solid-liquid surface energies range between 0.50191 (simulation 1a , 1b , 4 , 5 , 6 , 8), 0.57735 (simulation 2) and 1 (simulation 3). The different relative solid-solid to solid-liquid surface energies lead to different wetting angles and hence test the predictions of Bulau et al. (1979) or Laporte et al. (1997) concerning the shape of grains and melt pockets and their behavior at different wetting angles (simulations 1-3).

Numerical simulations

Different simulations have been performed using the same starting grain fabric but different relative surface energies and therefore different wetting angles. The starting configuration was taken from an in situ experiment of Walte et al. (2003) using norcamphor [Bons, 1992; Herwegh and Handy, 1996] as the rock analogue. In the presented simulations the relative solid-solid to solid-liquid surface energies have values that theoretically result in wetting angles of solid-liquid boundaries ranging between 10° and 120° if they are in equilibrium. In natural rocks, the observed wetting angles usually range between 10°-30° (e.g. [Laporte et al., 1997])while higher wetting angles only occur in case of a water-rich liquid phase.

Simulation 1a

In this simulation (Simulation 1a) relative solid-solid to solid-liquid surface energy ratios are such that the wetting angle is 10° at equilibrium. The melt fraction is fixed at 2%. The starting microstructure already shows some disequilibrium features, so that not all melt pockets have wetting angles of exactly 10°. However during the simulation grains quickly adjust to an equilibrium shape (convex triangle, E-shape) that is relatively stable. This behavior was predicted by Laporte et al. (1997) for wetting angles in a static system that are lower than 60° when grains have similar sizes.

Figure 1a. Relative solid-solid to solid-liquid surface energy ratios such that the wetting angle is 10° at equilibrium.

Relative solid-solid to solid-liquid surface energy ratios such that the wetting angle is 10° at equilibrium. The melt fraction is fixed at 2%. During the simulation grains quickly adjust to an equilibrium shape that is relatively stable, but continuous grain growth due to a reduction of the overall surface energy of the aggregate disturbs the equilibrium wetting angles.

However, continuous grain growth due to a reduction of the overall surface energy of the aggregate is disturbing the equilibrium wetting angles. This becomes obvious when small grains collapse completely.When the grains reach a certain critical size the total energy of their surfaces is relatively high because they have a very high surface curvature. Therefore they will dissolve or melt with an increasing velocity. Decreasing their size will just increase the surface curvature so that they will collapse completely in a relatively short time (relative to grain boundary movements of the other grains). During the collapse melt pockets are distorted and surrounding grains are bulging towards the disappearing grain until they are disconnected. The final collapse of the small grain leaves relatively large melt pockets (disequilibrium shape, D-shape). These disequilibrium structures disappear slowly (relative to their appearance) while the surrounding grains adjust their shape. Finally, melt pockets reappear that show the equilibrium shape and corresponding wetting angles.

The transition from an E-shaped to a D-shaped melt pocket increases its area and therewith its ratio of area to perimeter, forcing melt to be redistributed from other melt pockets into the D-shaped melt pocket. In Figure 3 the ratio of area vs. perimeter is shown for a single, D-shaped melt pocket and its changes over time during the simulation. Once the surrounding grains collapse, the D-shaped melt pocket splits into two convex triangles and the excess melt is redistributed to other E-shaped melt pockets.

Figure 3. Pictures of different stages during simulation 1a

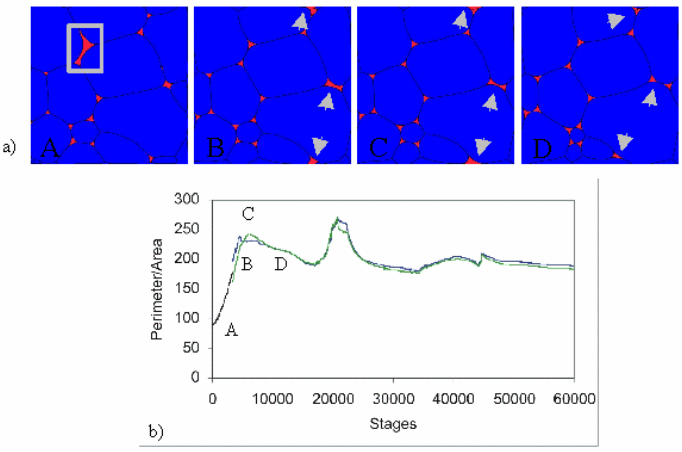

a. Pictures of different stages during simulation 1a. Location of observed D-shaped melt pocket in b) is outlined with gray square.

b. During the simulation, the are and the perimeter of the different melt pockets is calculated. The ratio of area to perimeter shown here corresponds to the melt pocket outlined in a) during the simulation. The initially black curve corresponds to the D-shaped melt pocket (located in A). In picture B, the initially E-shaped melt pocket split into two E-shaped melt pockets, the blue and green curves correspond to these E-shaped melt pockets. The peaks of the curves at 7000, 23000 and 45000 stages developed during the simulation at points where the formation or destruction of D-shaped melt pockets (see arrows in a) require the redistribution of melt.

The wetting angles of the melt pockets was initially set to 10°, but ranges between different values during the simulation. Especially during the formation of D-shaped melt pockets and the accompanying redistribution of melt, the E-shaped melt pockets display pronounced changes of their wetting angles. After destruction of the D-shaped melt pocket and accompanying redistribution of melt into the E-shaped melt pockets, the wetting angles tend to adjust again to 10°. This is in contrast to what was predicted from e.g. Laporteet al. (1997). It appears that the wetting angle cannot be treated as a constant parameter in short time periods. This also implies that the mean curvature of solid-liquid interfaces is not constant as was suggested by Laporte etal. (1997).

If the melt fraction is not fixed but allowed to grow, the melt pockets simply grow in size until no more solid grains exist. If the melt fraction is limited to a certain percentage, the melt pockets grow (or shrink) until the desired percentage is reached. The amount of melt introduced into the simulation has no influence on grain shape, noron the rate of development of the melt pockets (with the exception of unlimited melt where all the grains disappear).

Simulation 1b

In simulation 1b the melt pockets are surrounded by three regularly shaped grains so that the grains have an almost perfectly round shape. The melt pockets are distributed within the gussets of the grains. This simulates the grains having isotropic surface energies that are already minimized at the start of the simulation. The wetting angle is set to 10° and the melt fraction is fixed to the starting value. Since the surface energies of the grains is already minimal at the beginning of the simulation, no adjustment of the surface energies and therewith no change of shape of the crystals is necessary. Only where small distortions of the round grains occur (e.g. at the bottom of the simulation, because of the wrapping boundaries), the grains collapse and the melt pockets form a D-shape. Eventually this would continue throughout the whole area of the simulation since the distortions would work their way upward. However, it is clear that rounded (or spherical)shapes of the grains results in very little change of shapes of the melt pockets and surrounding grains and a very stable aggregate.

Figure 1b. Melt pockets are surrounded by three regularly shaped grains

Melt pockets are surrounded by three regularly shaped grains so that the grains have an almost perfectly round shape. The melt pockets are distributed within the gussets of the grains. This simulates the grains having isotropic surface energies that are already minimized at the start of the simulation.

Simulation 2 and Simulation 3

In simulation 2 and 3, the relative solid-solid to solid-liquid surface energies are set such that the wetting angle is 60° at equilibrium. The melt fraction is static at ~2%. The duration of the run is shorter than in the first simulation since equilibrium is reached much earlier. The boundaries of the E-shaped melt pockets straighten due to the higher wetting angle.A quick distribution of the melt into pockets at grain corners is observed and was predicted by [Bulau et al. (1979)].

Simulation 3 of a wetting angle of 120° showed the predicted results of [Bulau et al. (1979)]. At high wetting angles, the equilibrium shape of melt pockets is rectangular

and all the triangular shaped melt pockets disappear with their melt being redistributed into the rectangular shaped melt pockets. This behavior is completely due to the high wetting angle.

Figure 2. The relative solid-solid to solid-liquid surface energies is set such that the wetting angle is 60° at equilibrium

The relative solid-solid to solid-liquid surface energies is set such that the wetting angle is 60° at equilibrium. The melt fraction is static at ~2%. The duration of the run is shorter than in the first simulation since equilibrium is reached much earlier. The boundaries of the E-shaped melt pockets straighten due to the higher wetting angle.

Figure 3. The relative solid-solid to solid-liquid surface energies is set such that the wetting angle is 120° at equilibrium

The relative solid-solid to solid-liquid surface energies is set such that the wetting angle is 120° at equilibrium. At such high wetting angles, the equilibrium shape of melt pockets is rectangular and all the triangular shaped melt pockets disappear with their melt being redistributed into the rectangular shaped melt pockets.

Simulation 4, 5 and 6

In addition to the simulations described above, different parameters for the mobility of the respective boundaries were used in a set of simulations to analyze the influence of this parameter. The simulations show that variations of the mobility of the boundaries influences the velocity of the boundary-movement but have no impact on the resulting grain fabric or the equilibrium geometry of the melt pockets. All the simulations use the same starting grain fabric, surface energies and duration of simulation.The mobility of the boundaries was set to the highest (lowest) possible values or are equal. The movies shown below all have 25 frames per second so changes in the velocity of boundary movement are solely a result of the variations in the boundary mobility.

In simulation 4 , the mobility of the boundaries was set to be equal at 10^{-11}, in simulation 5 the mobility of the boundaries here was set to be equal at 1^{-10} and in simulation 6 the mobility of boundaries here was set to 1^{-10} for the ss boundaries and 1^{-11} for the sl boundaries.

Figure 4. The mobility of the boundaries set to 10-11

The mobility of the boundaries set to 10-11

Figure 5. The mobility of the boundaries set to 10-10

The mobility of the boundaries set to 10-10

Figure 6. The mobility of the boundaries set to 10-10 for the ss boundaries and 10-11 for the si boundaries

The mobility of the boundaries set to 10-10 for the ss boundaries and 10-11 for the si boundaries.

Analogue experiments

In situ analogue experiments have revealed that disequilibrium features can simply occur as a result of the combined effect of static liquid distribution with ongoing surface energy driven recrystallization [Walte et al. 2003]. For these analogue experiments a 30-100 µm thin sheet of norcamphor ($C_2H_{10}O$), a hexagonal organic crystal compound [Bons, 1992; Herwegh and Handy, 1996] plus ethanol liquid was placed between two glass slides and observed with a microscope under static conditions (see simulation 7). When surrounded by liquid the norcamphorforms circular crystals without crystal facets, therefore it has an effectively isotropic solid-liquid surface energy. The liquid is distributed within three-grain triple junctions with a mean dihedral angle of 10-15°. The norcamphor–ethanolsystem can therefore be used as an analogue for a low surface energy anisotropy phase plus a well wetting liquid or melt such as quartz plus granitic melt.The film shows that the melt triangles are regular as long as adjacent grains are rather equal sized. However, when a small grain shrinks and disappears, the melt filled triangles are distorted and temporarily form a disequilibrium feature.

The simulation of this experiment (see simulation 8) shows the same behavior of melt pockets.In both the analogue experiment and the simulation, the equilibrium is disturbed as soon as a grain collapses. During the collapse and during the formation of the disequilibrium shaped melt pockets, melt is redistributed and the wetting angles adjust so that the new volume of melt can be accommodated. If the disequilibrium melt pocket splits into two E-shaped melt pockets, melt is again redistributed and the wetting angle readjusts.

Figure 7. In situ analogue experiments

In situ analogue experiments of a norcamphor plus ethanol aggregate. The aggregate undergoes grain growth and develops the same disequilibrium structures during collapse of small grains that are seen in the numerical experiment. Simulation 8 is a numerical simulation

using the same initial microstructure that was used in the analogue experiments.

Figure 8. In situ analogue experiments

Simulation of the analogue experiment shown in animation 7. The simulation and the analogue experiment show the same behavior of melt pockets. In both the analogue experiment and the simulation, the equilibrium is disturbed as soon as a grain collapses.

Discussion

The simulations of melt processes on the grain scale have shown, that the most important parameter in the simulations is the relative surface energy and hence the wetting angle. If the surface energies in the simulations were chosen so that the wetting angle is high, the melt pockets tend to get straight or even concave boundaries before they quickly disappear, their melt being redistributed into large melt pockets. In simulation3 (wetting angle 120°) the large melt pockets are not triangular but resemble a distorted rectangle. The same holds true for the melt pockets in simulation 2 (wetting angle 60°), however, redistribution of melt into the larger melt pockets is much slower and the triangular shapes of melt pockets seems to be stable for a much longer period. Nevertheless, towards the end of the simulation all triangular melt pockets disappear and the melt is redistributed into the larger, rectangular shaped melt pockets towards the end of the simulation.

The triangular shaped melt pockets in simulation1a quickly adjust their ratio of circumference to area until they are stable (Figure 3). This includes a constant adjustment of the wetting angle at any given triple point because changes of the surrounding grains have to be accommodated. This change of the wetting angle also influences the mean curvature of boundaries between two triple points. The changes of the wetting angle can be quite large in case of melt being redistributed into D-shaped melt pockets. Only when the D-shaped melt pocket splits into two E-shaped melt pockets (in this case triangular) and melt is redistributed, the wetting angle is readjusted to approximately 10°. The same holds true for wetting angles in simulations 2 and 3. Therefore, the wetting angle (and hence the mean curvature of the melt pocket boundaries) during the simulations is not static but interactively adjusts to the loss or gain of melt and/or to the shapes of the surrounding grains.

Conclusions

The presented numerical modeling system Elle is capable of simulating melt processes at the grain scale. The results of the simulations comply with theoretical predictions on the behavior of melt in a (poly)crystalline aggregate. The most important parameters of the simulations are, apart from the starting grain fabric, the relative surface energies and hence the wetting angle. Different relative surface energies greatly influence the shape of the melt pockets during the simulation and, in contrast to the theoretical predictions, neither the wetting angle nor the mean curvature of a solid-liquid interface is static when observed over short periods of time. The change of the total energy of all surfaces and the accompanying redistribution of melt influences the wetting angle and the mean curvature at ss-sl interfaces. Only over geological time periods these parameters can be viewed as static.

If the starting grain fabric is chosen so that the grains approximate a sphere with melt located in the gussets between three grains, the surface energies are minimized and no change of the grain fabric occurs. In this case, small distortions of the shape of the grains leads to a small adjustment of the grain fabric. Whether this behavior influences the rheology of the rock by counteracting imposed changes due to deformation mechanisms is not yet clear and has to be investigated with further simulations.

The reason why the theoretical considerations fail to predict the disequilibrium features observed in the simulations as well as in the analogue experiments is the flawed assumption of a static equilibrium within a polycrystalline system. A solid–liquid system consisting of more than one crystal cannot be in real equilibrium and will always strive towards a lower total energy by surface energy driven grain coarsening, i.e. melt assisted recrystallization or Ostwald ripening at low and high melt fraction respectively. The observed formation and destruction of disequilibrium features in the analogue experiments and the simulations therefore show the complicated interaction of grain coarsening, which creates the disequilibrium features, and liquid dispersion, which counteracts disequilibrium liquid distribution.

Acknowledgments

This work was financially supported by the German Research Foundation (DFG), grant PA 578/6-1.

References

Bauer, P., Rosenberg, C., and Handy, M.R., 2000, "See-trough" deformation experiments on brittle-viscous norcamphor at controlled temperature, strain rate and applied confining pressure. J. Struct. Geol., 22, p. 281 - 289.

Bons, P.D., 1992, Experimental deformation of polyphaserock analogues. Geologica Ultraiectina, 110, 207 pp.

Bons, P.D., Jessel, M.W., Evans, L., Barr, T.D., and Stüwe K., 2001, Modelling of anisotropic grain growth in minerals. In:H.A. Koyi, N.S. Mancktelow (eds.): Tectonic modelling: A volume in honorof Hans Ramberg. Geol. Soc. Am. Mem., 193, p. 39 - 49.

Bulau, J.R., Waff, H.S., and Tyburczy, J.A., 1979, Mechanical and thermodynamical constraints on fluid distribution in partialmelts. J. Geophys. Res., 84, p. 6102-6108.

Cmiral, M., Fitz, G.J.D., Faul, U.H., and Green, D.H., 1998, A close look at dihedral angles and melt geometry in olivine-basalt aggregates; a TEM study. Contrib. Mineral. and Petrol., 130, 3 - 4, 336 –345.

Cooper, R.F., and Kohlstedt, D.L., 1984, Solution-precipitationenhanced enhanced diffusional creep of partially molten olivin-bassalt aggregates during hot pressing. Tectonophysics 107, p. 207 - 233.

Faul, U.H., 1997, Permeability of partially moltenupper mantle rocks from experiments and percolation theory. J. Geophys. Res., 102, p. 10299 - 10311.

Faul, U.H., 2001, Melt retention and segregation beneath mid-ocean ridges. Nature, 410, 6831, p. 920 - 923.

Herweg, M., and Handy, M.R., 1996, The evolution of high-temperature mylonitic microfabrics: Evidence from simple shearing of quartz analogue (norcamphor). J. Struct. Geol, 18, p. 689 - 710.

Hirth, G., and Kohlstedt, D.L., 1995, Experimental constraints on the dynamics of the partially molten upper mantle: Deformation in the diffusion creep regime. J. Geophys. Res., 100, p. 1981 - 2001.

Jessell, M., Bons, P., Evans, L., Barr, T., andStüwe, K., 2001, Elle: the numerical simulation of metamorphic and deformation microstructures. Computers and Geoscience, 27, p. 17 - 30.

Jung, H., and Waff, H.S., 1998, Olivine crystallographic control and anisotropic melt distribution in ultramafic partial melts. Geophys.Res. Letters, 25, 15, p. 2901 - 2904.

Jurewicz, S.R., and Watson, E.B., 1984, Distributionof partial melt in a felsic system; the importance of surface energy. Contrib.Mineral. and Petrol., 85, 1, p. 25 - 29.

Laporte, D., 1994, Wetting behavior of partial melts during crustal anatexis: The distribution of hydrous silicic melt inpolycrystalline aggregates of quartz. Contrib. Mineral. Petrol., 116, p.486 - 499.

Laporte, D., and Watson, E.B., 1995, Experimentaland theoretical constraints on melt distribution in crustal sources: theeffect of crystalline anisotropy on melt interconnectivity. Chemical Geol., 124, p. 161 - 184.

Laporte, D., Rapaille, C., and Provost, A., 1997, Wetting angles, equilibrium melt geometry, and the permeability threshold of partially molten crustal protoliths. In: Granite: From segregation of melt to emplacement fabrics, ed: Bouchez, J.L., Kluwer Academic Publishers1997.

Laporte, D., and Provost, A., 2000, The grain-scaledistribution of silicate, carbonate and metallosulfide partial melts: A review of theory and experiments. In: Bakssarov, N., (ed.): Physics and chemistryof partially molten rocks. Kluwer Academic Publications 2000.

McKenzie, D., 1984, The generation and compaction of partially molten rock. J. Petrol., 25, p. 713 - 765.

Park, Y., and Means, W.D., 1996, Direct observation of deformation processes in crystal mushes. J. Struct. Geol. 18, 847 - 858.

Rabinowicz, M., Genthon, P., Ceuleneer, G., and Hillairet, M., 2001, Compaction in a mantle mush with high concentrations and the generation of magma chambers. Earth and Planetary Sci. Let., 188, p. 313 - 328.

Rosenberg, C.L., and Handy, M.R., 2000, Syntectonicmelt pathways during simple shearing of a partially molten rock analouge(norcamphor-benzamide). J. Geophys. Res., 105, p. 3135 - 31349.

Scott, D.R., and Stevenson, D.J., 1986, Magma ascentby porous flow. J. Geophys. Res, 91, p. 9283 - 9296.

Sleep, N.H., 1988, Tapping of melt by veins anddykes. J. Geophys. Res., 93, p. 10255 - 10272.

Tullis, J., Christie, J.M., and Griggs, D.T., 1973, Microstructures and preferred orientations of experimentally deformed quarzites.Geol. Soc. Am. Bul, 84, p. 297 - 314.

von Bargen, N., and Waff, H.S., 1986, Permeabilities, interfacial areas and curvatures of partially molten systems: Results of numerical computations of equilibrium microstructures. J. Geophys. Res., 91, p. 9261 - 9276.

Waff, H.S., and Bulau, J.R., 1979, Equilibriumfluid distribution in an ultramafic partial melt under hydrostatic stress conditions. J. Geophys. Res., 84, p. 6109 - 6114.

Waff, H.S., and Faul, U.H., 1992, Effects of crystallineanisotropy on fluid distribution in ultramafic partial melts. J. Geophys.Res., 97, p. 9003 - 9014.

Walte, N.P., Bons, P.D., Passchier, C.W., and Koehn, D., 2003, Disequilibrium melt distribution during static recrystallization.Geology, 31, 11, p. 1009 - 1012.

Wark, D.A., Williams, C.A., Watson, E.B., and Price, J. D., 2003, Reassessment of pore shapes in microstructurally equilibrated rocks, with implications for permeability of the upper mantle. J. Geophys.Res. 108, B1, p. 12-1 - 12-16.